Exploring the limits of the Jenkinson-Collison classification scheme for atmospheric circulation: A global assessment based on various reanalyses

Juan Antonio Fernández-Granja (juan.fernandez@unican.es)
Universidad de Cantabria https://orcid.org/0000-0002-9763-7811

Swen Brands
Junta de Galicia: Xunta de Galicia

Joaquín Bedia
Universidad de Cantabria Escuela Técnica Superior de Ingenieros de Caminos Canales y Puertos: Universidad de Cantabria Escuela Tecnica Superior de Ingenieros de Caminos Canales y Puertos

Ana Casanueva
University of Cantabria: Universidad de Cantabria

Jesús Fernández
IFCA: Instituto de Fisica de Cantabria

Research Article

Keywords: Jenkinson-Collison classification, weather types, observational uncertainty, Transition Probabilities.

Posted Date: March 11th, 2022

DOI: https://doi.org/10.21203/rs.3.rs-1415588/v1

Exploring the limits of the Jenkinson-Collison classification scheme for atmospheric circulation: A global assessment based on various reanalyses

Juan A. Fernández-Granja[1*], Swen Brands[2], Joaquín Bedia[3], Ana Casanueva[3] and Jesús Fernández[1]

[1*]Meteorology Group, Instituto de Física de Cantabria (IFCA), Universidad de Cantabria-CSIC, Santander, 39005, Spain.
[2]MeteoGalicia, Consellería de Medio Ambiente, Territorio y Vivienda, Xunta de Galicia, Santiago de Compostela, Spain.
[3]Meteorology Group, Dept. of Applied Mathematics and Computer Science, Universidad de Cantabria, Santander, 39005, Spain.

*Corresponding author(s). E-mail(s): juan.fernandez@unican.es;
Contributing authors: swen.brands@gmail.com;
joaquin.bedia@unican.es; ana.casanueva@unican.es;
jesus.fernandez@unican.es;

Abstract

The Jenkinson-Collison weather typing scheme (JC-WT) is an automated method used to classify the regional atmospheric circulation into a reduced number of typical recurrent patterns, identified in the early 1970ies on the basis of expert knowledge. Originally developed for the British Isles, the method since then has seen many applications. Encouraged by the estimate that the JC-WT approach can in principle be applied to any mid-to-high latitude region (Jones et al, 2013), the present study explores whether it can be used anywhere in the extratropics, including the Southern Hemisphere. To this aim, JC-WT is applied at each grid-box of a global 2.5° regular grid excluding the inner tropics (± 5° band) where the method cannot be applied.

Thereby, 6-hourly JC-WT catalogues are obtained for 5 distinct reanalyses, covering the period 1979-2005, which are then applied to explore 1) the method's limits of applicability and 2) observational uncertainties inherent to reanalysis datasets. Using evaluation criteria such as the diversity of occurring circulation types and the frequency of unclassified situations, we extract empirically derived applicability thresholds which suggest that JC-WT can be generally used anywhere polewards of 22.5°. Seasonal variations compromise this finding along the equatorward limits of the domain, and so does the effect of large orographic barriers such as the Tibetan Plateau, the Andes, Greenland and Antarctica. In some regions, the JC-WT classifications obtained from the distinct reanalyses substantially differ from each other and this should be taken into account by further applications of the method.

Keywords: Jenkinson-Collison classification, weather types, observational uncertainty, Transition Probabilities.

1 Introduction

The large-scale atmospheric circulation exerts a direct influence on the regional climate. For instance, regarding the European climate, persistent high pressure (blocking) systems (Rex, 1950; Jury et al, 2019) or the North Atlantic Oscillation (NAO) pattern (Hurrell et al, 2003; Folland et al, 2009) are related to extreme seasonal temperature events (Buehler et al, 2011; Barriopedro et al, 2011; Favà et al, 2015; Schaller et al, 2018), wet spells and precipitation extremes (Busuioc et al, 2001; Casanueva et al, 2014; Sousa et al, 2017) or droughts (Bladé et al, 2011) due to their capability to disturb the predominant cyclonic westerly flow (Sillmann and Croci-Maspoli, 2009).

Similarly, in the South Hemisphere (SH), the Southern Annular Mode (SAM), also referred as the Antarctic Oscillation, influences the climate systems at high and middle latitudes (Gong and Wang, 1998, 1999; Thompson and Wallace, 2000; Thompson et al, 2000), displaying a 'seesaw' pattern for the atmospheric mass (SLP or geopotential heights). In essence, the SAM consists of a belt of strong westerly winds or low pressures surrounding Antarctica which exhibits a northward/southward displacement as its main mode of variability. For example, it is associated with storms and cold fronts that move from west to east largely determining precipitation in southern Australia (Stammerjohn et al, 2008; Risbey et al, 2009). Additionally, various modes of large-scale climate variability such as the El Niño-Southern Oscillation (ENSO), the Interdecadal Pacific Oscillation (IPO), the Indian Ocean Dipole (IOD), the Subtropical ridge (STR) or the Madden Julian Oscillation (MJO) largely determine the regional climate of the SH (Dey et al, 2019).

Hence, an adequate representation of atmospheric circulation and high-/low pressure variability becomes essential for a proper representation of the main regional climate features. In this context, synoptic weather types are a

useful tool as they summarize the whole range of variability of the data into a few, construable patterns (Huth et al, 1993, 2008; Littmann, 2000; Stryhal and Huth, 2017). A well-known circulation classification method is the Lamb Weather Type (LWT) Classification. The LWT classification is a subjective clustering approach created by the climatologist Hubert H. Lamb (Lamb, 1972) with the aim of studying the synoptic climatology over the British Isles. The system relies on a deterministic weather type classification based on a number of rules requiring meteorological expert knowledge for the interpretation of daily SLP charts, providing a straightforward and well defined physical interpretation of the atmospheric state. Later in the computer era, Jenkinson and Collison (1977) developed a more objective scheme following Lamb's principles, known as the Jenkinson-Collison weather type classification (JC-WT hereafter). The JC-WT approach is an automated procedure using a set of equations based upon sea level pressure (SLP) able to reproduce circulation types with negligible differences from the original LWT catalogue (Jones et al, 1993). Furthermore, unlike the original LWT approach, the JC-WT scheme has the advantage of being automatically applicable to different geographical locations through the introduction of some adjustment parameters to account for the relative grid spacing as a function of latitude.

The advantages of this circulation typing method has since then been exploited in different studies in the Northern Hemisphere (NH). For instance, JC-WTs have been centered in the Iberian Peninsula $[10°W, 40°N]$ (Trigo and DaCamara, 2000), $[5°W, 40°N]$ (Ramos et al, 2014), western Mediterranean basin $[5°E, 40°N]$ (Grimalt-Gelabert et al, 2013), southern Scandinavia $[15°E, 60°N]$ (Chen, 2000), south-west Russia $[55°E, 55°N]$ (Spellman, 2017), Ireland $[10°W, 55°N]$ (Fealy and Mills, 2018), Serbia $[20°E, 42.5°N]$ (Putnikovic et al, 2016), Central Europe $[10°E, 50°N]$ (Otero et al, 2018) and southeastern China (Wang and Sun, 2020; Wu et al, 2020). In an unprecedented study, Brands (2021) computed JC-WTs centered on every cell of the grid covering the majority of the NH extratropic region in order to evaluate GCM performance. The JC-WT classification has been seldom used in the southern hemisphere, excepting, to the best of our knowledge, by Sarricolea et al (2018) in southern Chile $[72.5°W, 42.5°S]$, requiring in this case an adaptation of the model equations to the SH circulation, as illustrated in this study.

The idea of evaluating model performance by means of atmospheric patterns and weather types started long time ago (Jones et al, 1993; Hulme et al, 1993), and the process-based evaluation paradigm has recently come into focus particularly within the downscaling community (Maraun et al, 2017), primarily aimed in this case at performing an optimal, objective selection of GCMs for downscaling experiments (Pickler and Mölg, 2021). Quoting Sterl (2004), 'if the pressure fields of two models differ, most other fields will differ too', which highlights the importance of SLP as the basic dynamical variable of a model and its relevance for model assessment. In this sense, model performance can be assessed by relying on SLP-based atmospheric circulation typing techniques such as the JC-WT classification, as an effective tool for model ranking and

selection (see e.g. Fernandez-Granja et al, 2021). Model evaluation involves the analytical comparison of model outputs against observations (or reanalysis, as pseudo-observations), taking into account that not only the model, but also the observations may be uncertain (Gettelman and Rood, 2016; Kotlarski et al, 2019). Most often, reanalysis products are used as reference, requiring a careful consideration of the divergence in their representation of climate features, particularly in regions where their background observational network has been historically sparse (Sterl, 2004; Lavin-Gullon et al, 2021) and those more sensitive to temporal non-stationarities in the assimilated data incorporated to the model by the observing systems (Bengtsson, 2004). As a result, it is widely recognized the need to consider multiple observational products when evaluating climate models (Gibson et al, 2019) and considerable effort has been devoted to the intercomparison of reanalysis products in different climate research contexts (e.g.: Chen et al, 2008; Ben Daoud et al, 2009; Brands et al, 2012) and the understanding of the underlying causes for their disagreement (Fujiwara et al, 2017).

This study describes an implementation of the JC-WT classification for its application worldwide, considering its adaptation to SH locations, and presents a 6-hourly database of JC-WT catalogues calculated from five different reanalysis products with a global coverage (excluding a 10°-width band along the equator). The objective is two-fold. First, we undertake an assessment of the JC-WT applicability across world regions, taking as reference the latest IPCC-WGI Reference Regions (Iturbide et al, 2020) for summarizing the results. These allow for the identification of the global areas where the JC-WT classification provides an effective tool for characterizing the atmospheric circulation. Second, we intercompare different JC-WT reanalysis catalogues with the aim of unveiling regions of high circulation uncertainty in the reanalyses. Caution is advocated in these areas, where the usage of more than one reanalysis is required in order to adequately evaluate the range of uncertainty in circulation-dependent modelling and/or downscaling exercises. The global JC-WT catalogues and the code implementing the worldwide JC-WT formulation used in this study are made available through dedicated Zenodo and GitHub open repositories.

2 Methodology and Data

2.1 Jenkinson-Collinson Classification

We follow the JC-WT formulation developed by Jenkinson and Collison (1977) that yields 27 different types. As input, we use 6-hourly, instantaneous sea level pressure (SLP) data, which are sampled using a cross-shaped point pattern (Fig. 1) formed by 16 points with a separation of 5° in latitude and 10° in longitude. Due to its shape, in the following, we will refer to this scheme simply as "cross". This cross can, in principle, be centered on any extra-tropical location.

The JC-WT classification is a function of 6 parameters related to wind-flow characteristics. Their corresponding equations are summarized in Table 1: southerly flow (S), westerly flow (W), total flow (F), southerly shear vorticity (Z_S), westerly shear vorticity (Z_W) and total shear vorticity (Z) computed upon the SLP records provided at a given time (6-hourly records in this study). The original parameter equations proposed by Jenkinson and Collison (1977) require further adjustments for their application in SH locations (Table 1). The result is a set of 27 weather types representing pure cyclonic (C) and anticyclonic (A) circulation over the center point, 8 pure directional types (N, NE, E, ..., NW), 16 hybrid types (mixing A or C with any of the directional types) and a 27th type accounting for unclassified records, that is, days with chaotic weak flow or days when incompatible hybrids are formed (Fig. 2). Equations for S, Z_W and Z_S use a number of adjustment coefficients (s, z_w^-, z_w^+, z_s) which take into account the relative grid spacing at different center latitudes (ψ, in degrees; Jones et al, 2013).

Param.	Northern hemisphere	Southern hemisphere	Wind-flow characteristics
W	$\frac{P_{12}+P_{13}}{2} - \frac{P_4+P_5}{2}$	$\frac{P_4+P_5}{2} - \frac{P_{12}+P_{13}}{2}$	Westerly flow
S	$s\left(\frac{P_5+2P_9+P_{13}}{4} - \frac{P_4+2P_8+P_{12}}{4}\right)$	$s\left(\frac{P_4+2P_8+P_{12}}{4} - \frac{P_5+2P_9+P_{13}}{4}\right)$	Southerly flow
D	$\arctan\frac{W}{S}$		Flow direction
F	$\sqrt{W^2+S^2}$		Resultant flow
Z_W	$z_w^-\left(\frac{P_{15}+P_{16}}{2} - \frac{P_8+P_9}{2}\right) - z_w^+\left(\frac{P_8+P_9}{2} - \frac{P_1+P_2}{2}\right)$	$z_w^+\left(\frac{P_1+P_2}{2} - \frac{P_8+P_9}{2}\right) - z_w^-\left(\frac{P_8+P_9}{2} - \frac{P_{15}+P_{16}}{2}\right)$	Westerly shear vorticity
Z_S	$z_s\left(\frac{P_6+2P_{10}+P_{14}}{4} - \frac{P_5+2P_9+P_{13}}{4} - \frac{P_4+2P_8+P_{12}}{4} + \frac{P_3+2P_7+P_{11}}{4}\right)$	$z_s\left(\frac{P_3+2P_7+P_{11}}{4} - \frac{P_4+2P_8+P_{12}}{4} - \frac{P_5+2P_9+P_{13}}{4} + \frac{P_6+2P_{10}+P_{14}}{4}\right)$	Southerly shear vorticity
Z	$Z_W + Z_S$		Total shear vorticity

where $s = \frac{1}{\cos\psi}$; $z_w^- = \frac{\sin\psi}{\sin(\psi-5°)}$; $z_w^+ = \frac{\sin\psi}{\sin(\psi+5°)}$; $z_s = \frac{1}{2\cos^2\psi}$

Table 1 Equations of the different circulation parameters of the JC-WT classification, for Northern and Southern Hemispheres. Fig. 1 displays the relative position of the points $i = 1, \ldots, 16$, where SLP values P_i are considered

In order to produce the classification for the entire globe, the center of the cross is displaced from one grid-box to another through all points of a reference 2.5° regular SLP grid within a band from 80°S to 80°N. Note that grid-boxes within 90°S − 80°S and 80°N − 90°N are beyond the range of the JC-WT method since the cross extends 10° north-south from its center (Fig. 1). The JC-WT method was conceived for extratropical application since significant pressure gradients within the cross, required for a meaningful classification, are expected to occur mainly in these latitudes. Consequently, the JC-WT domain of analysis is recommended to any mid-to-high latitude region (∼ 30° − 70°) by Jones et al (2013). However, in this study we calculate the JC-WT classification beyond these latitudes to obtain a more complete picture of the geographical limits of applicability of the method, also considering for the first time a spatially continuous application over the southern hemisphere.

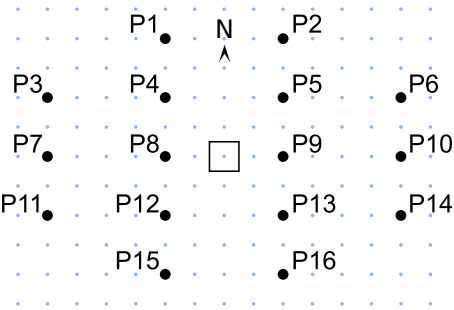

Fig. 1 Spatial distribution of the grid point pattern ("cross") of 16 points (in black) used in the JC-WT equations from Table 1. The background grid (in blue) represents the common, 2.5° regular grid, where the SLP has been interpolated. The square indicates the central grid cell of the cross, located at latitude ψ (see equations in Table 1).

Brands (2021) performs JC-WT classification over all cells but for the latitudes between 30° N and 70° N only. Note that the $z_w^{\mp}$ coefficients are undefined at $\psi = \pm 5°$ cross center latitudes (Table 1), and take nonphysical, negative values in between. Therefore, this latitudinal band has been excluded from our calculations.

The worldwide JC-WT method implementation here presented is available through the R package `transformeR` (v2.0.2, Iturbide et al, 2019). Its application is also illustrated through a worked example in the companion paper notebook (see Sec. *Availability of data and materials*).

2.2 Reanalysis data

We computed the global JC-WT classification using the 6-hourly SLP fields from five reanalysis products. Table 2 summarizes their features and provides references for further details. Prior to JC-WT application, all reanalyses were conservatively interpolated to a common 2.5° regular longitude-latitude grid (Fig. 1). In order to compare all reanalyses, we considered their common 27-year period 1979-2005, coincident with the AR5 CMIP5 historical baseline (Taylor et al, 2012). ERA-20C is produced through the assimilation of just SLP and marine winds, being therefore not fully comparable to the others, which assimilate a wider range of surface, upper-air and satellite observations. However, it has been also included in the intercomparison experiment for the sake of diversity. The reanalysis uncertainty is here analyzed by following an "all-against-all" validation scheme, so every reanalysis have been validated against each other.

2.3 Jenkinson-Collinson Classification assessment

2.3.1 Weather type frequencies and transition probabilities

One salient feature of a weather type is its probability of occurrence, which can be estimated by the relative frequency of occurrence in a sample, i.e. the proportion of 6-h records classified in a particular category over the complete

Reanalysis	Nom. res. (°)	Modelling Center	Reference
ERA-20C	1.13	ECMWF	Poli et al (2016)
ERA-Interim	0.75	ECMWF	Dee et al (2011)
ERA-5	0.25	ECMWF	Hersbach et al (2020)
JRA-55	1.25	JMA	Kobayashi et al (2015); Harada et al (2016)
NCEP Reanalysis 1	2.5	NCEP-NCAR	Kalnay et al (1996)

Table 2 Set of reanalyses used in this study, their nominal resolution at the equator (in °) and modelling centers producing them. ECMWF: European Center for Medium Range Weather Forecasts; JMA: Japanese Meteorological Agency; NCEP-NCAR: National Centers for Environmental Prediction / National Center for Atmospheric Research.

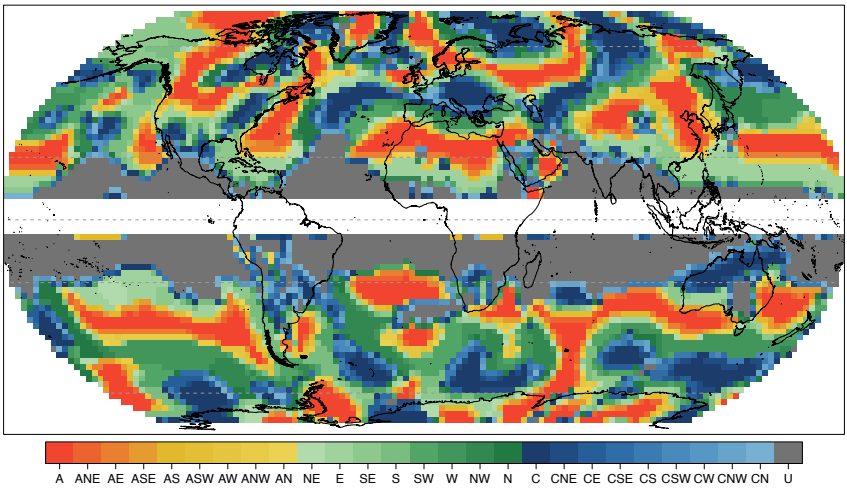

Fig. 2 Example of 6-hourly record of the Jenkinson-Collison Weather Type catalogue obtained from ERA-5, corresponding to the SLP state at 1979-01-01 00:00:00 UTC. The 26 JC-WT circulation types are indicated in the legend, ranging from purely anticyclonic (A) and its hybrids (ANE to AN), pure directional (NE to N) and purely cyclonic (C) and its hybrids (CNE to CN). Type 27, unclassified (U), is depicted in grey.

time series length. JC-WT persistence or, more generally, transition probabilities between two different types are also important. They determine key temporal features such as spell duration, serving as an effective tool for the assessment of the model ability to reproduce atmospheric circulation pattern sequences (Gibson et al, 2016; Hochman et al, 2019; Fernandez-Granja et al, 2021). In order to measure the differences among reanalyses, we assess both the JC-WT probabilities of occurrence for each individual type, as well as the probability of transition of one type into another. The latter are analysed using a transition probability matrix (TPM), briefly described next. Let the discrete random variable X_t represent a particular JC-WT at time t, whose values $x_t \in \{1, \ldots, K\}$, where $K = 27$ is the total number of WTs. We consider this

variable at two consecutive time steps, X_{t-1} and X_t, to construct the $K \times K$ transition probability matrix A, where $A_{ij} = p(X_t = j \mid X_{t-1} = i)$, representing the probability of transitioning from WT i to WT j. Hence, each row of the matrix sums to one, $\sum_j A_{ij} = 1$. The TPM thus provides a visual "fingerprint" on how a given dataset reproduces the JC-WT classification when centered on a given grid cell. TPMs can be compared to a reference through specific evaluation measures (Sec. 2.3.2). Further details and examples of TPM are presented in Fernandez-Granja et al (2021).

2.3.2 Evaluation measures

Two main aspects are addressed in our evaluation of the JC-WT classification. Firstly, we investigate the suitability of the method for each world region by using two criteria: (1) the number of different types, measuring the regional circulation's *diversity*, and (2) the occurrence of the Unclassified (U) type, witnessing weak pressure gradient with no clear vorticity tendency, also known as *barometric swamp* (Grimalt-Gelabert et al, 2013). Low diversity and frequent barometric swamp are here assumed to be indicative of the method working at its theoretical limits, i.e. in climate regimes for which it has not been developed; most prominently the monsoon and Intertropical Convergence Zone. Applying the method under these circumstance makes little sense since synoptic variability is either missing at the considered scale, is represented by other variables than SLP. We here intentionally push the method to its limits in order to explore whether it can be applied anywhere in between 30 and 70 degrees North or South, as was estimated by Jones et al (2013), or even beyond. For the diversity criterion, we consider weather types attaining relative frequencies above 0.1%, i.e. 40 or more occurrences in the total record of nearly 40,000 time steps. This threshold has been chosen since some JC-WTs were found to occur with relative frequencies as small as 0.47% in its original formulation for the British Isles (Perry and Mayes, 1998). In light of both measures (weather type diversity and type U frequency) jointly considered, we aim to obtain empirical evidence about the global geographical boundaries for the applicability of the JC-WT classification.

Secondly, reanalysis uncertainty is addressed. In order to evaluate the discrepancies among reanalyses, we measure the differences in their resulting JC-WT classification considering the relative bias of their WT frequencies, as well as the statistical significance of these differences using a two-proportions Z-test. Annual and seasonal relative biases for each WT are computed among all pairs of reanalyses in Table 2. The relative bias is a non-dimensional measure, which is zero for a perfect agreement of frequencies. The null hypothesis for the two-proportions Z-test is that the relative frequencies of a given type for two different reanalyses are the same. We use this parametric test in order to identify significant differences in their resulting weather type frequencies. Here, we use the Z-test implementation in the `prop.test` function from the R package `stats` (v3.6.3, R Core Team, 2020), which includes an exact test

for small samples, better suited for infrequent weather types. The test was performed using a 95% confidence level.

Reanalysis differences in their representation of transition probabilities were evaluated by the TPM Score (TPMS, eq. 1), envisaged to provide a quantitative measure of dissimilarity between two transition probability matrices (Fernandez-Granja et al, 2021). TPMS is defined as follows:

$$TPMS = \sum_{p \in A^*} \mid p - p_{ref} \mid \tag{1}$$

where p and p_{ref} are the transition probabilities in the test and in the reference datasets, respectively. The (absolute) difference is calculated considering a subset of transition probabilities A^* from the full matrix (A), that are significantly different between the two reanalyses considered in each comparison, following the two-proportion Z-test. In order to include the "missing" transitions in the score (i.e. either transitions that exist in the reference but do not occur the test dataset, or transitions that occur in the test but do not in the reference dataset), these are assigned a zero probability (i.e. either $p = 0$ or $p_{ref} = 0$) and included in the A^* subset. As a result, the larger the TPMS departure from zero (perfect agreement), the larger the dissimilarity of the TPM fingerprints between the reanalyses for a given center grid cell.

2.4 Regional synthesis

Finally, in order to provide a synthetic overview of the main results, we provide a regional assessment of our results. To this aim, we use the latest set of climatic reference regions used in by the IPCC for the assessment of historical trends and future climate change projections (Iturbide et al, 2020). In order to avoid the inclusion of unsuitable areas for the application of the JC-WT methodology and provide a more meaningful summary valid for regional intercomparison purposes, we exclude from the original polygon dataset the whole intertropical range, thus producing a modification of some of the original IPCC regions to exclude this area. The IPCC regions affected are indicated with an asterisk throughout the text. The modified polygon layer is included as supplementary material of this study to ensure the reproducibility of the results (see Sec. *Availability of data and materials*).

3 Results and discussions

3.1 Suitability of the JC-WT classification worldwide

For brevity, the following results are based on ERA-5 unless otherwise indicated. The global distribution of the total number of distinct WTs (Fig. 3, left) shows a marked latitudinal gradient, with a decreasing diversity of types towards the tropics. Conversely, the frequency of the U type (Fig. 3, right) exhibits a sudden increase in the tropics, following a pattern similar to type

diversity (left). In general, the lower the diversity of types, the higher the frequency of the U type, with a few regional exceptions, where reduced diversity coincides with small U numbers. Such exceptions are found *year-round* over Antarctica and the Tibetan Plateau; and to a lesser degree also over Greenland and the southern Indian Ocean at mid-latitudes. During JJA season, the Mediterranean, Middle-East and southwestern United States can be added to this list, as well as the mid-latitude eastern South Atlantic and eastern South Pacific for DJF.

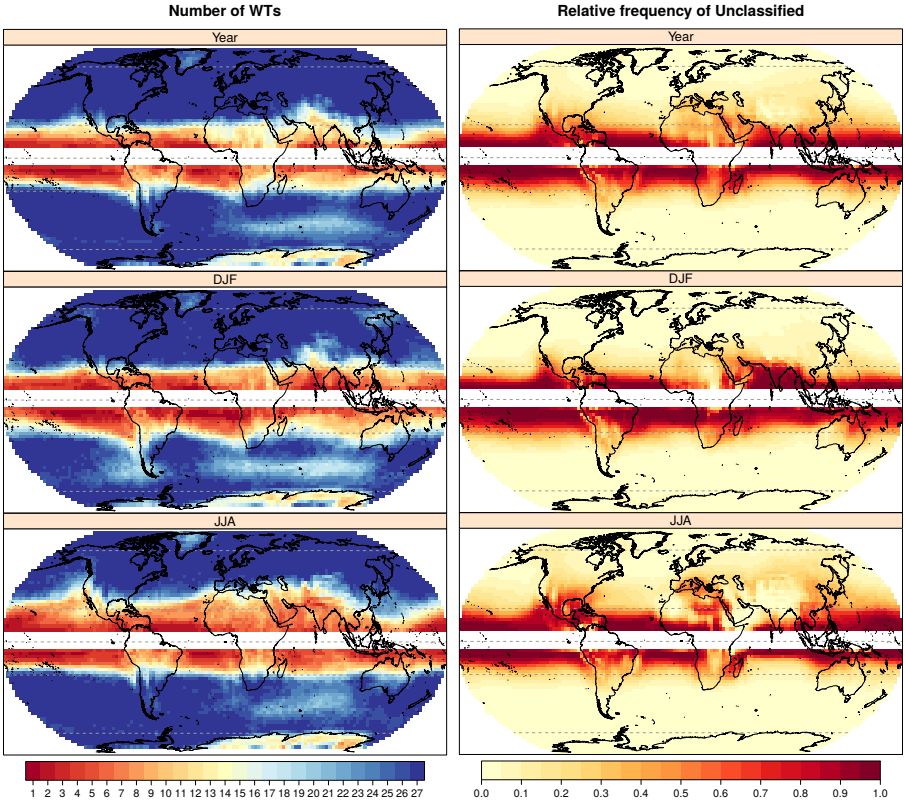

Fig. 3 Summary of the Jenkinson-Collison global classification calculated upon the SLP from ERA-5 (6-hourly, 1979-2005), considering the whole annual series (top row) and DJF and JJA seasons (rows 2–3 respectively). Left column: Number of weather types per grid-box with a relative frequency above 0.1%, DJF and JJA. Right column: Relative frequency of the Unclassified type (U) per grid-box.

Visual inspection of the maps in Fig. 3 reveals a remarkable empirical threshold of around 16 different types coinciding with at least half the temporal record falling into the U type. This threshold will be interpreted as applicability criterion in the forthcoming and is generally met polewards of 22.5° latitude on both hemispheres, which clearly extends the range of application suggested by Jones et al (2013), from 30° to 70°.

The aforementioned thresholds exhibit seasonal excursions that go hand in hand with the seasonal shifts of the Intertropical Convergence Zone (ITCZ, Barry and Carleton, 2013), where local scale processes of deep convection are predominant. This seasonal fluctuations of the ITCZ may alter to some extent the applicability of the JC-WT classification even in the extra-tropics. In the Mediterranean Basin, for instance, suitability is optimal during DJF (boreal winter, maximum JC-WT diversity and a negligible type U frequency), which is due to a southward shift of the Atlantic storm tracks in combination with autochthonous cyclogenesis over the Mediterranean Sea (Fita et al, 2007). In JJA (boreal summer), however, the U type frequency increases in hand with a shrinking type diversity, hence compromising the usefulness of the classification during this season. On both hemispheres, the favourable area widens towards the equator during their winter and retreats towards the respective pole during summer (Fig. 3).

3.2 Reanalysis Uncertainty

After determining the regional applicability limits of the JC-WT classification, we next analyze its consistency among different reanalyses. In order to summarize the results, we will here refer to the modified IPCC-AR6 regions (Sec. 2.4, Fig. 4).

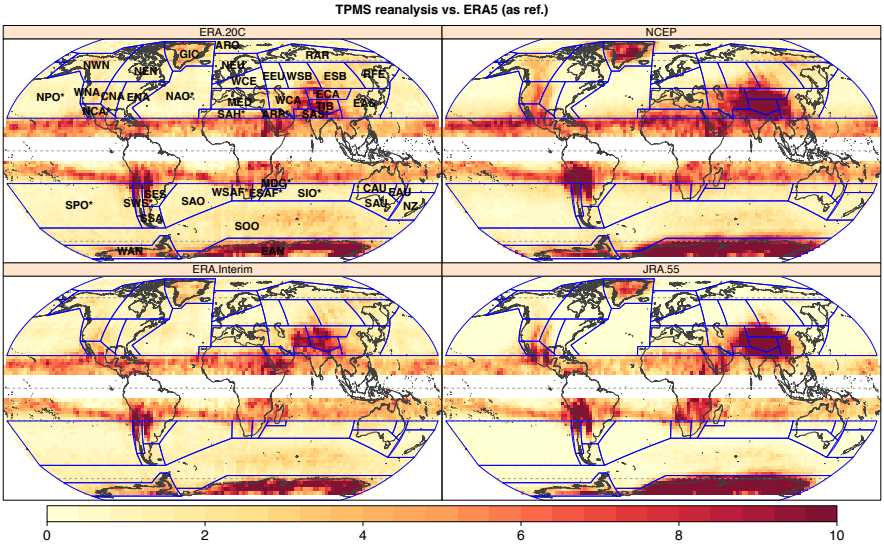

Fig. 4 Annual Transition Probability Matrix Scores (TPMS, Sec. 2.3.2) of NCEP, ERA-Interim, ERA-20C and JRA-55 against ERA-5 (used as reference). The modified IPCC region polygon layer with the region identification codes are depicted in the top-left. Note that the original IPCC regions that have been modified to exclude the intertropical range (see Sec. 2.4) are marked with an asterisk.

In terms of TPMS, ERA-20C and ERA-Interim are generally more similar to ERA-5 (Fig. 4) than NCEP and JRA-55. For the latter two datasets, particularly large TPMS values are obtained over Greenland (GIC), Western North America (WNA), the central Asian regions (ECA, EAS), northern India (SAS*) and the Tibetan Plateau (TIB), where values in excess of 10 are found. In the Southern Hemisphere, large discrepancies between the applied reanalyses are found over South America (SWS* and SES regions). Interestingly, these mentioned regions present complex orography, with high-altitude mountain systems such as the Himalayas, the Andes and the Rockies mountain; and big ice sheets like the Antarctic and Greenland. These results are in line with Sterl (2004), who found large differences between NCEP and ERA-40 (Simmons and Gibson, 2000) reanalyses in these areas. This observational uncertainty still remains after the development of newer reanalysis products and it is likely related to the different algorithms used to reduce surface pressure to mean sea level. Differences due to different algorithms can reach several hPa (Fita et al, 2019). The better coherence of the results in high-altitude regions from all ECMWF reanalyses (ERA-20C, ERA-Interim and ERA5; see Fig. A1), despite their different resolution and model generation, supports this hypothesis. In the Northern Hemisphere, Brands (2021) found similar results when comparing the atmospheric circulation of JRA-55 and ERA-Interim, even when using a different metric (Mean Absolute Error, MAE). That study shows a general agreement between reanalyses, with exceptions in high-orography regions such as Greenland, the Tibetan Plateau or North-Central America (results of TPMS JRA-55 versus ERA-Interim in Figure A1 in the Appendix). Additionally, another previous study also found that there are differences in the deep convection represented by ERA-Interim, JRA55 and NCEP over La Plata basin. More precisely, a low pressure area favoured by a trough located in southern Bolivia that contributes to the extension of the South American Low-Level Jet southward (Lavin-Gullon et al, 2021). This is in accordance with the large TPMS found in the northwards grid-boxes of SWS* and SES. The mentioned study also speculates that the complex orography of the Andes and surrounding areas is not sufficiently well represented by the coarse resolution of the reanalysis ($\sim$ 75 km) and causes these discrepancies.

The seasonal analysis of the TPMS between JRA-55 and ERA-5 (Fig. 5) generally reveals a seasonal march of the larger values towards the pole of the summer hemisphere. This is similar to the results found for type diversity and U frequency (Sect. 3.1), where the ITCZ may determine the JC-WT applicability to some point in that oscillating stripe.

In particular, the seasonal TPMS values for North Central-America (NCA*) and the Sahara region (SAH*) are larger than the annual ones (Fig. 5). In the Mediterranean (MED) and in West North-America (WNA), the TPMS values are largest in JJA and lowest in DJF. Reflecting the aforementioned seasonal march, the TPMS values for South South-America (SSA), West South-Africa (WSAF*), East South-Africa (ESAF*), Madagascar (MDG*)

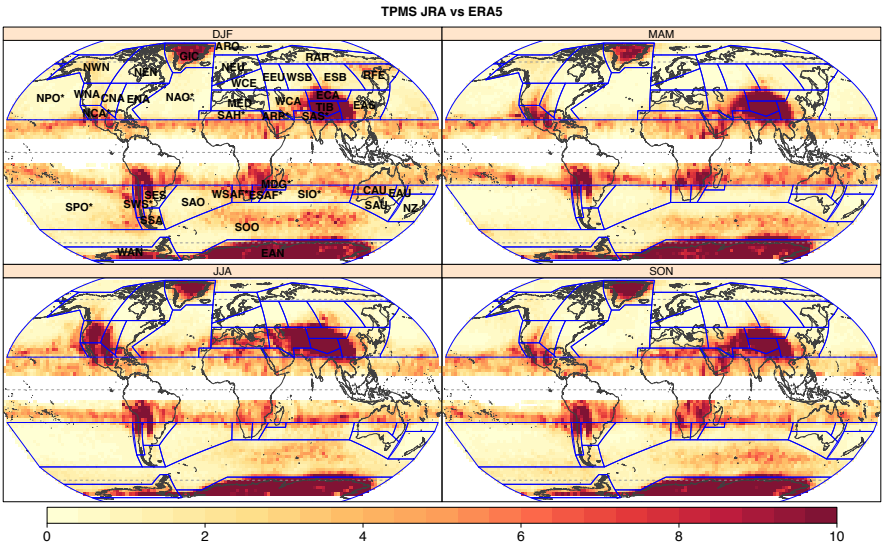

Fig. 5 Seasonal Transition Probability Matrix Scores (TPMS, Sec. 2.3.2) of JRA-55 reanalysis against ERA-5 (reference).

and Central Australia (CAU) reach their maximum in DJF, with a much larger magnitude than in any other season.

According to Fig. 5, moderately high TPMS values are found year-round in the mid-latitude Indian Ocean, which extend to the eastern South Atlantic and eastern South Pacific during DJF (austral summer), particularly affecting the Southern-Ocean (SOO) region. These differences might be caused by scarce observations in that area and, noteworthy, they again coincide with a relatively low type diversity, as reported in the previous section.

The large TPMS values found along the margins of the East Antarctic Ice Sheet (EAIS) are probably related to an abrupt shift of the easterly katabatic winds blowing down the ice sheet to quasi-persistent westerlies at mid-latitudes, driving the Antarctic Ocean divergence zone (Davis and McNider, 1997). This singular regional modulation of the wind field might by resolved in a distinct manner by the two reanalyses and so is the pressure reduction to mean sea-level over the ice sheet itself. Notably, the TPMS values over the West Antarctic Ice Sheet are systematically lower than those over the EAIS (compare WAN to EAN regions respectively).

In order to shed some light on regional TPMS, we investigate the relative biases of each WT for each IPCC region, which reveals misrepresentations of the synoptic conditions and their frequencies by the applied reanalyses. As an illustrative example, we show the results for MED region in Fig. 6. The respective results for the remaining IPCC regions can be obtained by following the working example on analysis reproducibility indicated in Sec. *Availability of data and materials*.

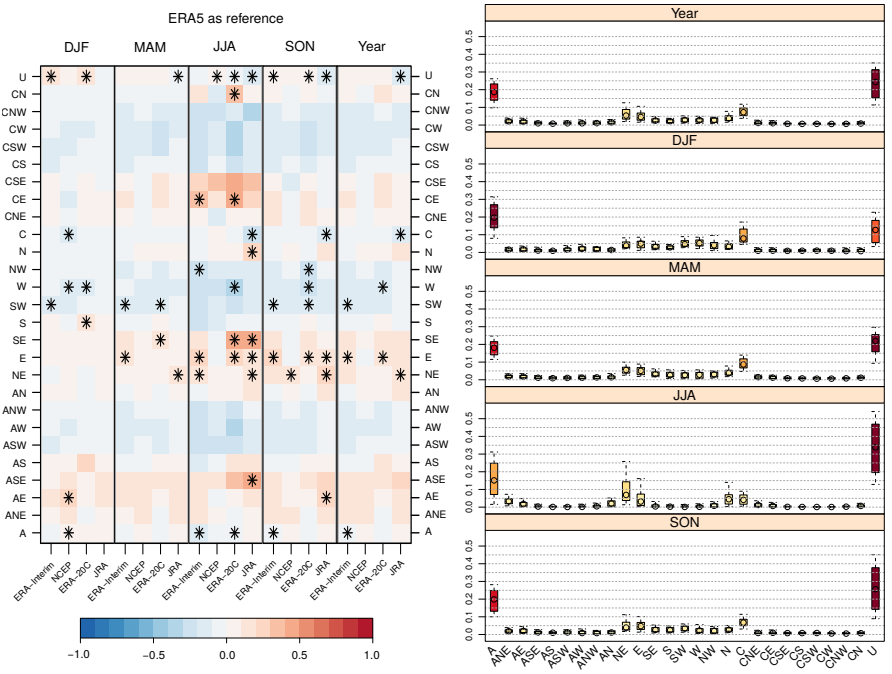

Fig. 6 Left: Annual and seasonal relative biases of weather type frequencies for the different reanalyses (in columns) against ERA-5 (reference) for MED. Asterisks indicate statistically significant differences following the two proportion Z-test (Sec. 2.3.2). Right: Annual and seasonal regional weather type frequencies as represented by ERA-5 for MED, used as reference for the relative biases on the left. The boxes represent the spatial variability of type frequencies within MED, where the box upper/lower boundaries show the inter-quartile range and the lower/upper whiskers extend to the 10^{th} and 90^{th} percentiles respectively. Circles indicate the median frequency.

The results show biases of different magnitude and sign, depending on the reanalysis. The majority of statistically significant differences (marked with asterisks) occur for the most frequent WTs (according to WTs frequencies in the right panel). The largest and most significant biases are found during JJA, which coincides with large TPMS values (Fig. 5). For the least frequent weather types, the reanalyses do not exhibit significant differences with respect to ERA5, especially in spring, autumn and for the annual results. The Unclassified type is the most frequent one in all seasons except DJF. It exhibits significant differences among reanalyses in all seasons, especially during JJA and SON.

All in all, we found a relationship between three factors, namely large values of TPMS (Figs. 4 and 5), small number of WTs and high frequency of the U type (Fig. 3). TPMS and number of WTs should be analyzed together due to the fact that large TPMS in some regions might come from the limitations in the suitability of the WT classification. In other regions where the classification method is more suitable, the TPMS purely reflects the uncertainly among

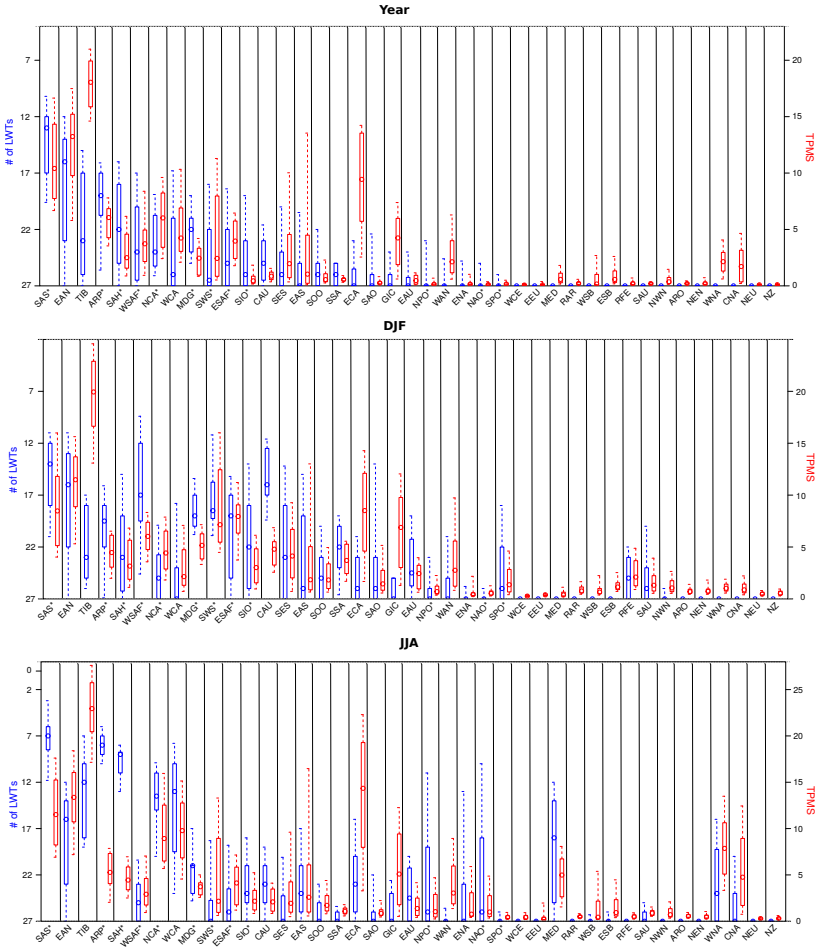

Fig. 7 TPMS (in red) of JRA-55 against ERA-5 and the number of WTs (in blue) of ERA-5 for each IPCC region. The three different panels correspond to annual, DJF and JJA. The limits of the boxes show the spatial interquartile range and whiskers depict the 10^{th} and 90^{th} percentile. The median values are represented with a circle inside the boxes. In the three panels, regions are sorted by decreasing order of the 75^{th} percentile of the number of WTs at annual scale.

reanalyses. However, the relationship seems to be clearer among large TPMS and low number of LWTs. Fig. 7 summarizes Figs. 3, 4 and 5 for all the IPCC regions and analizes the connection between the number of distinct WTs and TPMS.

Considering the criteria of JC-WT diversity, the method might be less suitable for regions like SAS* and EAN, where few distinct WTs appear (median below 16 types). Seasonally, other regions also stand out by their low number of WTs, e.g. CAU or WSAF* in boreal winter and TIB, ARP*, SAH*, NCA* and WCA in boreal summer (Fig. 7). There is a large spatial variability in terms

of WTs diversity in some regions where the applicability of the WT classification is questionable, such as EAN, TIB, ARP*, SAH* or WSAF*. Regardless of their median number of WTs, these regions show grid cells where all WTs are registered. Additionally, there are some regions that stand out for having large TPMS (i.e. reanalysis uncertainty) despite of their large number of WTs: EAN, NCA*, SWS*, ESAF*, SES, EAS, ECA and GIC; only in DJF we can add TIB, SSA and WAN; and only in JJA we can add MED, WNA and CNA.

4 Conclusions

In the present study, we assess the potential applicability of JC-WT classification for any region of the world except the inner tropics and explore to which extent the frequencies and transitions probabilities of the 27 classes obtained from several reanalyses agree with each other. To this end, we first formulate a modification of JC-WT method to allow for its use in the Southern Hemisphere and then use two different criteria to evaluate its applicability worldwide: the number of LWTs reflecting "type diversity" and the relative frequency of the Unclassified type. A roll-out of up to 41 regions extracted from the latest set of IPCC Working Group I reference regions has been used to divide the globe in order to address these analyses on the regional scale. Five different reanalysis products are taken into account to assess reanalysis uncertainty by means of the TPMS and relative bias. They cover different producing centers, spatial resolutions and reanalysis generations.

As a main result, the JC-WT approach can be generally applied anywhere within 22.5° and 80° on both hemispheres, excluding the East Antarctic Ice Sheet. This clearly exceeds the estimate made by Jones et al (2013), who argued that the method should be applicable in mid-to-high latitudes ($\sim 30°$ to 70°). For a large fraction of this new recommended area, the majority of WTs occur with a reasonable frequency while the number of unclassified time steps is acceptable. The isoline of *sixteen* types occurring with a reasonable frequency is located just in the area of largest spatial gradients for both *type diversity* and the frequency of *unclassified* time steps.

Both the 16-types isoline and the area of large TPMS values, indicating enhanced reanalysis uncertainty, exhibit a seasonal march towards the pole of the respective summer hemisphere. This excursion is particularly strong during JJA (boreal summer) and seems to be associated with the ITCZ, along which converging winds trigger deep convection on a scale not captured by the JC-WT approach.

Within the newly defined area where the JC-WT approach is found to be applicable, a general agreement between the employed reanalyses is observed in terms of the *annual* TPMS. On the one hand, there are regions where the JC-WT approach is in principle applicable whereas its practical use is hampered by large reanalysis differences. These are SWS*, ECA, GIC, MED, WNA and NCA* regions in JJA, as well as the TIB, MDG*, SWS*, ESAF*,

ECA, and GIC regions in DJF. On the other hand, there are regions where JC-WT is less suitable irrespective of the obtained reanalysis uncertainty. These are the SAS*, EAN, TIB, ARP*, SAH*, NCA*, and WCA regions in JJA, the SAS*, EAN, WSAF* and CAU regions in DJF and the SAS* and EAN regions throughout all seasons of the year.

Another aspect is that ERA-20C, ERA-Interim and ERA5 represent more similarly the transition probabilities among WTs than NCEP and JRA-55, specially in areas of complex orography. Large inhomogeneities among reanalyses occur over high-altitude regions, such as the Tibetan plateau, the Andes and Rockies mountain ranges or the Antarctic and Greenland ice sheets. Similar differences are found in previous studies for these regions. Sterl (2004) found large differences between NCEP and ERA-40 (Simmons and Gibson, 2000) in GIC, EAN, TIB and SWS. These uncertainties are still present in the recent reanalysis products. Lavin-Gullon et al (2021) identify differences in the synoptic mechanisms represented by ERA-Interim, JRA55 and NCEP over La Plata basin, which are in line with the large TPMS found in SWS* and SES and supports our hypothesis of the role of deep convection on the TPMS. In Brands (2021), where the JC-WT approach is applied in a latitudinal range following the recommendation in Jones et al (2013), similar results were obtained when comparing the JC-WTs of JRA-55 and ERA-Interim despite using a different evaluation measure. The agreement of our results with the results from Brands (2021) may favour our proposed extension of the WT classification algorithm and the usability of TPMS as a robust evaluation metric.

Acknowledgments. We thank our colleague Prof. A. S. Cofiño for guidance in scientific metadata handling.

Declarations

Funding. This paper is part of the R+D+i projects CORDyS (PID2020-116595RB-I00) and ATLAS (PID2019-111481RB-I00), funded by MCIN/AEI/10.13039/501100011033. J.A.F. has received research support from grant PRE2020-094728 funded by MCIN/AEI/10.13039/501100011033. J.B. and A.C. received research support from the project INDECIS, part of the European Research Area for Climate Services Consortium (ERA4CS) with co-funding by the European Union (grant no. 690462).

Competing Interests. The authors declare no competing interests

Authors' contributions. J.A.F., S.B., J.B. and A.C. designed the experiments and J.A.F. carried them out by developing, debugging and running the experiment code. J.F was also crucial for the interpretation, illustration and discussion of the results. J.A.F prepared the manuscript with contributions from all co-authors.

Availability of data and materials. The JC-WT method implementation used in this study is available in open climate4R package transformeR https:

//doi.org/10.5281/zenodo.3839618. We provide further reproducible examples of the methods and figures in a paper notebook available in the public GitHub repository at https://github.com/SantanderMetGroup/notebooks (`2021_JC_Worldwide_suitability.*` files).

The JC-WT catalogues and the IPCC regions shape-files are published in Zenodo (https://doi.org/10.5281/zenodo.5761257)

Appendix A Remaining TPMS among reanalyses

The remaining pairs of TPMS among reanalyses can be found in Fig. A1.

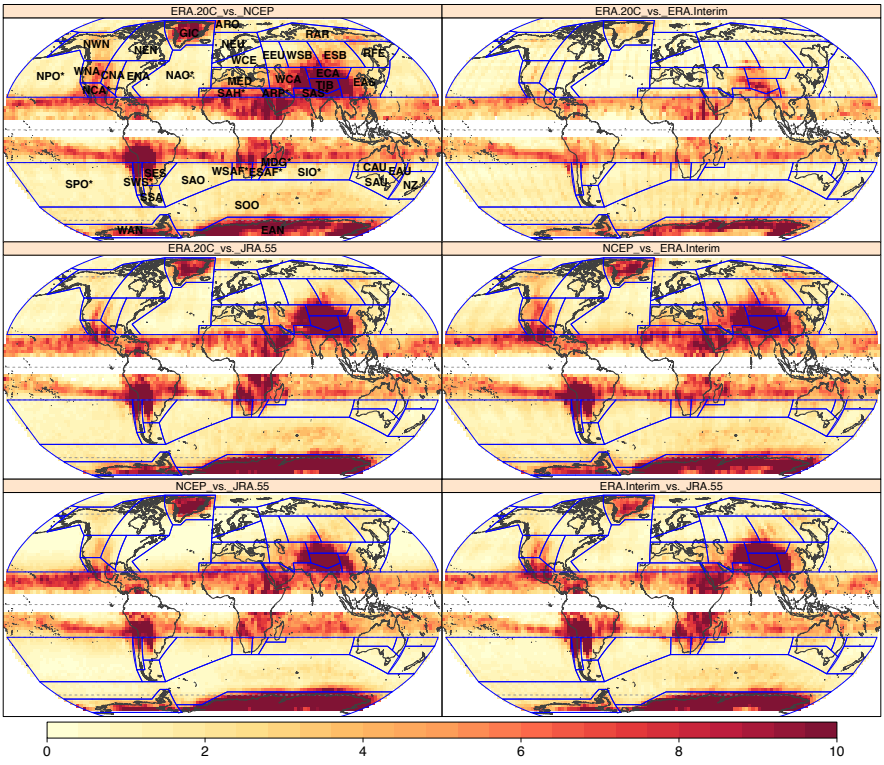

Fig. A1 Annual TPMS among different reanalyses (specific pairs are found in the sub-panels titles). IPCC regions short names can be seen in the top-left sub-panel.

References

Barriopedro D, Fischer EM, Luterbacher J, et al (2011) The Hot Summer of 2010: Redrawing the Temperature Record Map of Europe. Science 332(6026):220–224. https://doi.org/10.1126/science.1201224

Barry RG, Carleton AM (2013) Synoptic and dynamic climatology. Routledge

Ben Daoud A, Sauquet E, Lang M, et al (2009) Comparison of 850-hPa relative humidity between ERA-40 and NCEP/NCAR re-analyses: detection of suspicious data in ERA-40. Atmospheric Science Letters 10(1):43–47. https://doi.org/10.1002/asl.208, URL https://hal-insu.archives-ouvertes.fr/insu-00411903

Bengtsson L (2004) Can climate trends be calculated from reanalysis data? Journal of Geophysical Research 109(D11):D11,111. https://doi.org/10.1029/2004JD004536, URL http://doi.wiley.com/10.1029/2004JD004536

Bladé I, Liebmann B, Fortuny D, et al (2011) Observed and simulated impacts of the summer NAO in Europe: implications for projected drying in the Mediterranean region. Climate Dynamics 39(3-4):709–727. https://doi.org/10.1007/s00382-011-1195-x

Brands S (2021) A circulation-based performance atlas of the cmip5 and 6 models for regional climate studies in the northern hemisphere. Geoscientific Model Development Discussions 2021:1–48. https://doi.org/10.5194/gmd-2020-418, URL https://gmd.copernicus.org/preprints/gmd-2020-418/

Brands S, Gutiérrez JM, Herrera S, et al (2012) On the use of reanalysis data for downscaling. Journal of Climate 25(7):2517 – 2526. https://doi.org/10.1175/JCLI-D-11-00251.1, URL https://journals.ametsoc.org/view/journals/clim/25/7/jcli-d-11-00251.1.xml

Buehler T, Raible CC, Stocker TF (2011) The relationship of winter season North Atlantic blocking frequencies to extreme cold or dry spells in the ERA-40. Tellus A: Dynamic Meteorology and Oceanography 63(2):174–187. https://doi.org/10.1111/j.1600-0870.2010.00492.x

Busuioc A, Chen D, Hellström C (2001) Performance of statistical downscaling models in GCM validation and regional climate change estimates: application for Swedish precipitation: STATISTICAL DOWNSCALING FOR SWEDISH PRECIPITATION. International Journal of Climatology 21(5):557–578. https://doi.org/10.1002/joc.624

Casanueva A, Rodríguez-Puebla C, Frías MD, et al (2014) Variability of extreme precipitation over europe and its relationships with teleconnection patterns. Hydrol Earth Syst Sci 18(2):709–725. https://doi.org/10.5194/

hess-18-709-2014

Chen D (2000) A monthly circulation climatology for sweden and its application to a winter temperature case study. International Journal of Climatology 20:1067–1076. https://doi.org/10.1002/1097-0088(200008)20:103.0.CO;2-Q

Chen J, Del Genio AD, Carlson BE, et al (2008) The Spatiotemporal Structure of Twentieth-Century Climate Variations in Observations and Reanalyses. Part I: Long-Term Trend. Journal of Climate 21(11):2611–2633. https://doi.org/10.1175/2007JCLI2011.1, URL http://journals.ametsoc.org/doi/10.1175/2007JCLI2011.1

Davis A, McNider R (1997) The development of antarctic katabatic winds and implications for the coastal ocean. Journal of the atmospheric sciences 54(9):1248–1261

Dee DP, Uppala SM, Simmons AJ, et al (2011) The ERA-Interim reanalysis: configuration and performance of the data assimilation system. Q J R Meteorol Soc 137:553–597. https://doi.org/10.1002/qj.828

Dey R, Lewis SC, Arblaster JM, et al (2019) A review of past and projected changes in australia's rainfall. Wiley Interdisciplinary Reviews: Climate Change 10(3):e577

Favà V, Curto JJ, Llasat MC (2015) Relationship between the summer NAO and maximum temperatures for the Iberian Peninsula. Theoretical and Applied Climatology pp 1–15. https://doi.org/10.1007/s00704-015-1547-2

Fealy R, Mills G (2018) Deriving lamb weather types suited to regional climate studies: A case study on the synoptic origins of precipitation over ireland. International Journal of Climatology https://doi.org/10.1002/joc.5495

Fernandez-Granja JA, Casanueva A, Bedia J, et al (2021) Improved atmospheric circulation over europe by the new generation of cmip6 earth system models. Climate Dynamics 56. https://doi.org/10.1007/s00382-021-05652-9

Fita L, Romero R, Luque A, et al (2007) Analysis of the environments of seven mediterranean tropical-like storms using an axisymmetric, nonhydrostatic, cloud resolving model. Natural Hazards and Earth System Sciences 7(1):41–56. https://doi.org/10.5194/nhess-7-41-2007, URL https://nhess.copernicus.org/articles/7/41/2007/

Fita L, Polcher J, Giannaros TM, et al (2019) CORDEX-WRF v1.3: development of a module for the Weather Research and Forecasting (WRF) model to support the CORDEX community. Geoscientific Model Development 12(3):1029–1066. https://doi.org/10.5194/gmd-12-1029-2019

598 Folland CK, Knight J, Linderholm HW, et al (2009) The Summer North
599 Atlantic Oscillation: Past, Present, and Future. Journal of Climate
600 22(5):1082–1103. https://doi.org/10.1175/2008JCLI2459.1

601 Fujiwara M, Wright JS, Manney GL, et al (2017) Introduction to the sparc
602 reanalysis intercomparison project (s-rip) and overview of the reanalysis
603 systems. Atmospheric Chemistry and Physics 17(2):1417–1452. https://doi.
604 org/10.5194/acp-17-1417-2017, URL https://acp.copernicus.org/articles/
605 17/1417/2017/

606 Gettelman A, Rood RB (2016) Model Evaluation. In: Gettelman A, Rood
607 RB (eds) Demystifying Climate Models: A Users Guide to Earth System
608 Models. Earth Systems Data and Models, Springer, Berlin, Heidelberg,
609 p 161–176, https://doi.org/10.1007/978-3-662-48959-8_9, URL https://doi.
610 org/10.1007/978-3-662-48959-8_9

611 Gibson PB, Uotila P, Perkins-Kirkpatrick SE, et al (2016) Evaluating synoptic
612 systems in the cmip5 climate models over the australian region. Climate
613 Dynamics 47(7):2235–2251

614 Gibson PB, Waliser DE, Lee H, et al (2019) Climate Model Evaluation in
615 the Presence of Observational Uncertainty: Precipitation Indices over the
616 Contiguous United States. Journal of Hydrometeorology 20(7):1339–1357.
617 https://doi.org/10.1175/JHM-D-18-0230.1, URL http://journals.ametsoc.
618 org/doi/10.1175/JHM-D-18-0230.1

619 Gong D, Wang S (1998) Antarctic oscillation: concept and applications.
620 Chinese Science Bulletin 43(9):734–738

621 Gong D, Wang S (1999) Definition of antarctic oscillation index. Geophysical
622 research letters 26(4):459–462

623 Grimalt-Gelabert M, Tomas-Burguera M, Alomar-Garau G, et al (2013)
624 Determination of the jenkinson and collison's weather types for the west-
625 ern mediterranean basin over the 1948-2009 period: Temporal analysis.
626 Atmosfera 26:75–94. https://doi.org/10.1016/S0187-6236(13)71063-4

627 Harada Y, Kamahori H, Kobayashi C, et al (2016) The jra-55 reanalysis:
628 Representation of atmospheric circulation and climate variability. Jour-
629 nal of the Meteorological Society of Japan Ser II 94(3):269–302. https:
630 //doi.org/10.2151/jmsj.2016-015

631 Hersbach H, Bell B, Berrisford P, et al (2020) The era5 global reanalysis.
632 Quarterly Journal of the Royal Meteorological Society 146(730):1999–2049

633 Hochman A, Alpert P, Harpaz T, et al (2019) A new dynamical systems
634 perspective on atmospheric predictability: Eastern mediterranean weather

regimes as a case study. Science Advances 5(6):eaau0936. https://doi.org/10.1126/sciadv.aau0936

Hulme M, Briffal K, Jones P, et al (1993) Validation of gcm control simulations using indices of daily airflow types over the british isles. Climate Dynamics 9(2):95–105. https://doi.org/https://doi.org/10.1007/BF00210012

Hurrell JW, Kushnir Y, Ottersen G, et al (2003) An overview of the North Atlantic Oscillation. In: Hurrell JW, Kushnir Y, Ottersen G, et al (eds) Geophysical Monograph Series, vol 134. American Geophysical Union, Washington, D. C., p 1–35

Huth R, Nemesova I, Klimperová N (1993) Weather categorization based on the average linkage clustering technique: An application to european mid-latitudes. International Journal of Climatology 13(8):817–835. https://doi.org/10.1002/joc.3370130802

Huth R, Beck C, Philipp A, et al (2008) Classifications of atmospheric circulation patterns: Recent advances and applications. Annals of the New York Academy of Sciences 1146:105–152. https://doi.org/10.1196/annals.1446.019

Iturbide M, Bedia J, Herrera S, et al (2019) The R-based climate4R open framework for reproducible climate data access and post-processing. Environmental Modelling & Software 111:42–54. https://doi.org/10.1016/j.envsoft.2018.09.009

Iturbide M, Gutiérrez JM, Alves LM, et al (2020) An update of ipcc climate reference regions for subcontinental analysis of climate model data: definition and aggregated datasets. Earth System Science Data 12(4):2959–2970. https://doi.org/10.5194/essd-12-2959-2020, URL https://essd.copernicus.org/articles/12/2959/2020/

Jenkinson A, Collison F (1977) An initial climatology of gales over the north sea. synoptic climatology branch memorandum. Meteorological Office, 62

Jones PD, Hulme M, Briffa KR (1993) A comparison of Lamb circulation types with an objective classification scheme. International Journal of Climatology 13(6):655–663. https://doi.org/10.1002/joc.3370130606

Jones PD, Harpham C, Briffa KR (2013) Lamb weather types derived from reanalysis products. International Journal of Climatology 33(5):1129–1139. https://doi.org/10.1002/joc.3498

Jury MW, Herrera S, Gutiérrez JM, et al (2019) Blocking representation in the ERA-Interim driven EURO-CORDEX RCMs. Climate Dynamics 52(5-6):3291–3306. https://doi.org/10.1007/s00382-018-4335-8

672 Kalnay E, Kanamitsu M, Kistler R, et al (1996) The NCEP/NCAR 40-
673 Year Reanalysis Project. Bulletin of the American Meteorological Society
674 77(3):437–472. https://doi.org/10.1175/1520-0477(1996)077⟨0437:TNYRP⟩
675 2.0.CO;2, publisher: American Meteorological Society

676 Kobayashi S, Ota Y, Harada Y, et al (2015) The jra-55 reanalysis: General
677 specifications and basic characteristics. Journal of the Meteorological Society
678 of Japan Ser II 93(1):5–48. https://doi.org/10.2151/jmsj.2015-001

679 Kotlarski S, Szabó P, Herrera S, et al (2019) Observational uncertainty and
680 regional climate model evaluation: A pan-European perspective. Interna-
681 tional Journal of Climatology 39(9):3730–3749. https://doi.org/10.1002/joc.
682 5249, URL https://onlinelibrary.wiley.com/doi/10.1002/joc.5249

683 Lamb H (1972) British isles weather types and a register of daily sequence of
684 circulation patterns 1861-1971. Meteorological Office, Geophysical Memoir
685 116:1–85

686 Lavin-Gullon A, Feijoo M, Solman S, et al (2021) Synoptic forcing associ-
687 ated with extreme precipitation events over southeastern south america
688 as depicted by a cordex fps set of convection-permitting rcms. Climate
689 Dynamics 56(9):3187–3203

690 Littmann T (2000) An empirical classification of weather types in the mediter-
691 ranean basin and their interrelation with rainfall. Theoretical and Applied
692 Climatology 66(3-4):161–171. https://doi.org/10.1007/s007040070022

693 Maraun D, Shepherd TG, Widmann M, et al (2017) Towards process-informed
694 bias correction of climate change simulations. Nature Climate Change
695 7(11):664–773. https://doi.org/10.1038/nclimate3418

696 Otero N, Sillmann J, Butler T (2018) Assessment of an extended version of
697 the jenkinson–collison classification on cmip5 models over europe. Climate
698 Dynamics 50. https://doi.org/10.1007/s00382-017-3705-y

699 Perry A, Mayes J (1998) The lamb weather type cata-
700 logue. Weather 53(7):222–229. https://doi.org/https://doi.
701 org/10.1002/j.1477-8696.1998.tb06387.x, URL https://rmets.
702 onlinelibrary.wiley.com/doi/abs/10.1002/j.1477-8696.1998.tb06387.x,
703 https://arxiv.org/abs/https://rmets.onlinelibrary.wiley.com/doi/pdf/10.1002/j.1477-
704 8696.1998.tb06387.x

705 Pickler C, Mölg T (2021) General Circulation Model Selection Technique for
706 Downscaling: Exemplary Application to East Africa. Journal of Geophysi-
707 cal Research: Atmospheres 126(6). https://doi.org/10.1029/2020JD033033,
708 URL https://onlinelibrary.wiley.com/doi/10.1029/2020JD033033

Poli P, Hersbach H, Dee DP, et al (2016) ERA-20C: An atmospheric reanalysis of the twentieth century. Journal of Climate 29(11):4083–4097. https://doi.org/10.1175/JCLI-D-15-0556.1

Putnikovic S, Tosic I, Durdevic V (2016) Circulation weather types and their influence on precipitation in serbia. Meteorology and Atmospheric Physics 128. https://doi.org/10.1007/s00703-016-0432-6

R Core Team (2020) R: A Language and Environment for Statistical Computing. R Foundation for Statistical Computing, Vienna, Austria, URL https://www.R-project.org/

Ramos AM, Cortesi N, Trigo RM (2014) Circulation weather types and spatial variability of daily precipitation in the Iberian Peninsula. Frontiers in Earth Science 2. https://doi.org/10.3389/feart.2014.00025

Rex DF (1950) Blocking Action in the Middle Troposphere and its Effect upon Regional Climate. Tellus 2(3):196–211. https://doi.org/https://doi.org/10.1111/j.2153-3490.1950.tb00331.x

Risbey JS, Pook MJ, McIntosh PC, et al (2009) On the remote drivers of rainfall variability in australia. Monthly Weather Review 137(10):3233–3253

Sarricolea P, Meseguer-Ruiz O, Martin-Vide J, et al (2018) Trends in the frequency of synoptic types in central-southern chile in the period 1961–2012 using the jenkinson and collison synoptic classification. Theoretical and Applied Climatology 134. https://doi.org/10.1007/s00704-017-2268-5

Schaller N, Sillmann J, Anstey J, et al (2018) Influence of blocking on Northern European and Western Russian heatwaves in large climate model ensembles. Environmental Research Letters 13(5):054,015. https://doi.org/10.1088/1748-9326/aaba55, URL https://iopscience.iop.org/article/10.1088/1748-9326/aaba55

Sillmann J, Croci-Maspoli M (2009) Present and future atmospheric blocking and its impact on European mean and extreme climate. Geophysical Research Letters 36(10):L10,702. https://doi.org/10.1029/2009GL038259

Simmons A, Gibson J (2000) The era-40 project plan. Tech. Rep. 1, ECMWF, Shinfield Park, Reading, URL https://www.ecmwf.int/node/12272

Sousa PM, Trigo RM, Barriopedro D, et al (2017) Responses of European precipitation distributions and regimes to different blocking locations. Climate Dynamics 48(3-4):1141–1160. https://doi.org/10.1007/s00382-016-3132-5

Spellman G (2017) An assessment of the jenkinson and collison synoptic classification to a continental mid-latitude location. Theoretical and Applied

Climatology 128. https://doi.org/10.1007/s00704-015-1711-8

Stammerjohn SE, Martinson DG, Smith RC, et al (2008) Trends in antarctic annual sea ice retreat and advance and their relation to el niño–southern oscillation and southern annular mode variability. Journal of Geophysical Research: Oceans 113(C3). https://doi.org/https://doi.org/10.1029/2007JC004269, URL https://agupubs.onlinelibrary.wiley.com/doi/abs/10.1029/2007JC004269, https://arxiv.org/abs/https://agupubs.onlinelibrary.wiley.com/doi/pdf/10.1029/2007J

Sterl A (2004) On the (In)Homogeneity of Reanalysis Products. Journal of Climate 17(19):3866–3873. https://doi.org/10.1175/1520-0442(2004)017⟨3866:OTIORP⟩2.0.CO;2, URL https://journals.ametsoc.org/view/journals/clim/17/19/1520-0442_2004_017_3866_otiorp_2.0.co_2.xml, publisher: American Meteorological Society Section: Journal of Climate

Stryhal J, Huth R (2017) Classifications of Winter Euro-Atlantic Circulation Patterns: An Intercomparison of Five Atmospheric Reanalyses. Journal of Climate 30(19):7847–7861. https://doi.org/10.1175/JCLI-D-17-0059.1, URL https://doi.org/10.1175/JCLI-D-17-0059.1, https://arxiv.org/abs/https://journals.ametsoc.org/jcli/article-pdf/30/19/7847/4768338/jcli-d-17-0059_1.pdf

Taylor KE, Stouffer RJ, Meehl GA (2012) An overview of cmip5 and the experiment design. Bulletin of the American Meteorological Society 93(4):485–498. https://doi.org/10.1175/BAMS-D-11-00094.1

Thompson D, Wallace J (2000) Annular modes in the extratropical circulation. part i: Month-to-month variability. Journal of Climate 13:1000–1016. https://doi.org/10.1175/1520-0442(2000)01360;1000:amitec62;2.0.co;2

Thompson D, Wallace J, Hegerl G (2000) Annular modes in the extratropical circulation. part ii: Trends. J Climate 13:1018–1036. https://doi.org/10.1175/1520-0442(2000)013⟨1018:AMITEC⟩2.0.CO;2

Trigo RM, DaCamara CC (2000) Circulation weather types and their influence on the precipitation regime in Portugal. International Journal of Climatology, p 23. https://doi.org/10.1002/1097-0088(20001115)20:13%3C1559::AID-JOC555%3E3.0.CO;2-5

Wang Y, Sun X (2020) Weather type classification and its relation to precipitation over southeastern china. International Journal of Climatology https://doi.org/10.1002/joc.6747

Wu J, Li C, Ma Z, et al (2020) Influence of meteorological conditions on ozone pollution at shangdianzi station based on weather classification. Huanjing kexue 41:4864–4873. https://doi.org/10.13227/j.hjkx.202003307